Advanced Steel Construction – Vol. 20 No. 1 (2024) 53–59
DOI:10.18057/IJASC.2024.20.1.6

STUDY ON FLEXURAL CAPACITY OF PROFILED STEEL SHEET - POLYURETHANE SANDWICH SLABS

Wen-Tao Qiao [1, 2, *], Zhi-Yuan Huang [1], Teng Wang [3], Kai-Li Cui [1] and Li-Jun Meng [1]

[1] *School of Civil Engineering, Shijiazhuang Tiedao University, Shijiazhuang, China*
[2] *Key Laboratory of Roads and Railway Engineering Safety Control (Shijiazhuang Tiedao University), Ministry of Education, Shijiazhuang, China*
[3] *State-owned Enterprise Comprehensive Service Center of Ningjin County Finance Bureau, Xingtai, China*
** (Corresponding author: E-mail: qwt@stdu.edu.cn)*

ABSTRACT

Widely employed in enveloped structures, the metal-faced sandwich panel boasts thermal insulation, noise abatement, lightweight, and remarkable assembly efficiency. In this paper, a new type of profiled steel sheet and polyurethane sandwich slab (PSSPSS) was proposed. Through static load tests and numerical simulations, the flexural properties of the PSSPSS were studied, and the influence of individual geometric parameters on the flexural capacity of the structure was evaluated. The results of this analysis led to the derivation of the calculation formulas for the deflection and flexural bearing capacity of the PSSPSS. These results demonstrate that the bearing capacity and failure mode of the structure, as determined by test and simulation, are in perfect agreement. The sandwich slab's failure is mainly demonstrated by an overabundance of deflection, with the peak being 1/42 of the span, and the channel steel at the middle span being distorted and snapped. The slab deflection calculation formula's results, when compared to the test results, demonstrate a mere 2.1% error, thus confirming its accuracy. The slab thickness, profiled steel sheet thickness, polyurethane foam density, and slab span all contribute to higher bearing capacity and improved stiffness in the structure, yet the effect of the slab span is more evident. The slab span, however, has a more profound effect on stiffness. The flexural bearing capacity formula's applicability is indicated by the maximum error being within 10%, as demonstrated by the comparison of the formula's results with the FEA results for the sandwich slab with varying parameters.

ARTICLE HISTORY

Received: 18 May 2023
Revised: 11 October 2023
Accepted: 18 November 2023

KEYWORDS

Sandwich slab;
Channel steel;
Profiled steel sheet;
Polyurethane foam;
Flexural capacity

1. Introduction

Under the dual influence of policy guidance and market demand, various new prefabricated building systems have been proposed[1]. Now, sandwich slabs with metal materials as panels are widely used in the construction field due to their unique structure and excellent combination performance. Among them, the metal surface layer has a protective effect on the core layer, preventing it from weathering, avoiding mechanical damage, and isolating water and water vapor. The core layer can connect the two surface layers as a whole and bear the load together. When the surface layer is buckling under load, the core layer can support the surface layer and increase the buckling resistance of the surface layer, and it also has the functions of heat insulation and sound insulation[2].

Metal panels and a variety of lightweight core materials have become the ideal materials for wall panels and roof panels due to their remarkable combination advantages. Some scholars have researched the metal-faced sandwich panels and put forward relevant design theories. Noor. A.K. et al.[3] proposed three analytical models that are commonly used in the study of mechanical properties of sandwich panels. The first one is a simplified model, which is often used to solve the problems of panel wrinkles. The second one is a two-dimensional model based on Reissner theory, Hough theory, and Polushakov-Duqing Hua theory, and the two-dimensional model is more accurate and widely used. The third is a three-dimensional and quasi-three-dimensional continuum model, which uses an equivalent homogeneous segmented anisotropic body to replace panels and cores, and the analysis is the most sophisticated but also the most complex. Y.H. Mugahed. et al.[4,5] carried out a theoretical analysis on the extremes of fully composite and non-composite action of sandwich slabs and proposed a typical analysis method to determine the degree of composite action. Jongchol Choe. et al.[6-8] proposed a new one-dimensional layered model that uses Euler Bernoulli beam theory in the skin and higher-order kinematics in the core, this model can efficiently and accurately characterize the critical load and post-buckling behavior of sandwich structures. Aktham. et al.[9] proposed the FEA method for sandwich slabs under eccentric loading. Hartsock. J. A. and Chong. K. P. et al.[10-12] took the single-span simply-supported sandwich panel under uniform load and mid-span concentrated load as the research object, analyzed the bending deformation and internal force calculation, and compared with the test results, which were in good agreement. On this basis, Allen[13,14] proposed the calculation method of the mechanical properties of sandwich plates under uniform load and concentrated load. Sohel[15,16] proposed a theoretical model to predict the flexural and punching resistance and a good correlation with test results is obtained. A large deflection analysis considering plate membrane action is also proposed to predict the force-deflection relation of Steel-Concrete-Steel sandwich slabs. In addition, based on the theoretical analysis model proposed by the above scholars, some scholars have carried out a lot of analysis and research on the mechanical properties of sandwich structures and proposed different calculation models. Davies. J. M.[17-19] conducted a large number of finite element analyses on the pressed metal panel sandwich slab, and successively proposed the finite element analysis method of the bending performance of the sandwich slab and the combined action of bending and compression. The sandwich panel was divided into two parts, the flange and the core layer. The core part considered the bending deformation and shear deformation of the core, while the flange part ignored the shear deformation of the flange and only considered its bending deformation. The formula of mid-span deflection of single-span sandwich panels under uniform load and concentrated load is obtained by this approximate calculation method. Chong and Hartsoek[20] proposed and summarized the structural behavior of sandwich slabs, including flexural stresses, deflections, vibration, and thermal stresses. Russo and Zuccarello[21] carried out experimental and numerical evaluation of the mechanical behavior of sandwich structures, constituted by fiber-glass laminate skins over PVC foam or polyester mat cores. Ramtekka et al.[22,23] studied the application of a three-dimensional mixed finite element model to the flexure of a sandwich plate. Kachalla.[24,25] proposed a new method to analyze the longitudinal bearing capacity of composite slabs based on the partial shear method and the European code. Besides, Davies and Hakmi studied on local buckling behavior of foam-filled thin-walled steel sandwich beams using the effective width concept. There have been some other studies on the axial load-bearing behavior of sandwich composite panels[26-29]. In summary, a large number of studies have been conducted on the bearing capacity and deformation of sandwich roof panels and wall panels mainly through experimental research, numerical simulation, and theoretical analysis. However, due to the low bearing capacity and poor stiffness, metal-faced sandwich panels are rarely used on floors.

In view of the advantages, a new type of assembled sandwich slab structure is proposed in this paper, that is, based on the structure of metal-faced sandwich panels, the double-layer deep profiled steel sheet and channel steel are combined, and the rigid polyurethane foam material is filled as the core of the sandwich panel. In this paper, the flexural bearing capacity and parameter influence of PSSPSS were studied using experiment and finite element simulation analysis. On this basis, the calculation formulas of deflection and flexural bearing capacity of the sandwich slab were derived.

2. Structure of the slab

PSSPSS is mainly composed of profiled steel sheets, channel steel, and rigid polyurethane foam. Based on the structure of metal faced sandwich slab, the channel steel is used as the frame, the double-layer deep profiled steel plate

is used as the metal panel, and the rigid polyurethane foam material is used as the core layer of the sandwich slab. The structure of the sandwich slab is shown in Fig. 1**.**

As one of the materials with the best thermal insulation performance, rigid polyurethane foam can effectively improve the thermal insulation performance of the floor. At the same time, in the process of polyurethane foaming, the core material will automatically bond and firmly adhere to the surface layer, eliminating the procedure of spraying adhesives. In addition, the utilization of channel steel as the foundation of the floor slab not only enhances the bearing capacity and bending rigidity of the floor slab; but also facilitates the connection between the floor and the wall in assembly.

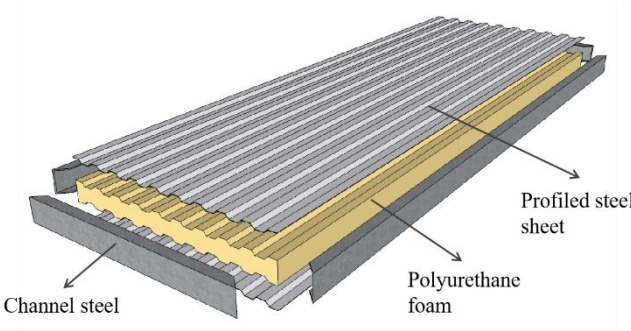

Fig. 1 Sandwich slab structure diagram

3. Experimental studies

3.1. Test specimen

In the test, a full-scale PSSPSS test piece with dimensions of 4100mm×1200mm×140mm is designed and produced. Q235 steel is the source of the profiled sheet, which is 2mm in thickness, and [14a is the channel steel. The section characteristics of the specimen are shown in Fig.2.

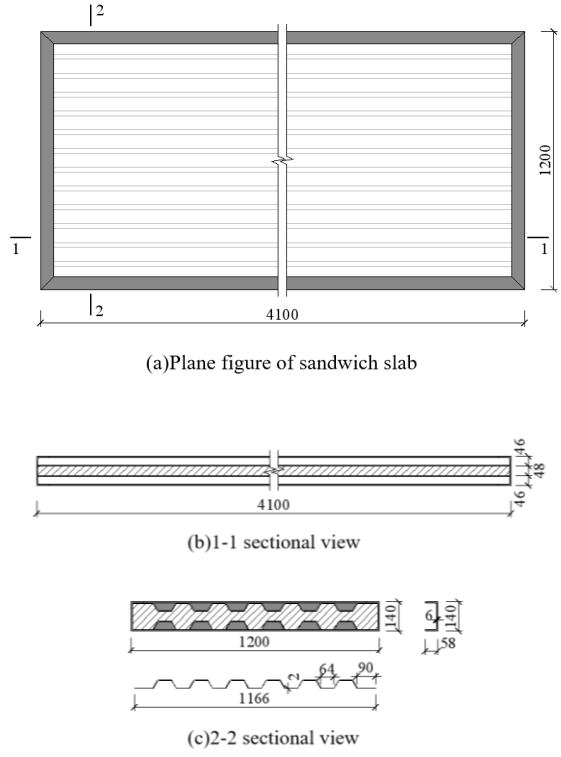

Fig. 2 Section characteristics and size of the sandwich slab

3.2. Material properties

The samples of the steel material are taken from the same batch of steel as the specimen. The steel is divided into hot-rolled steel and cold-formed steel, and each steel is divided into three groups. According to the Chinese specification GB/T228.1 - 2010[30], the tensile tests are carried out on the steel samples of steel sheet and channel steel. The test results are shown in Table 1 and Fig. 3.

Table 1
Summary of material properties

Specimen	Yield strength/MPa	Tensile strength/MPa
SS-1	270	360
SS-2	273.8	365
SS-3	277.5	370
Average	273.75	365
CS-1	282	376
CS-2	273.75	365
CS-3	287.25	383
Average	281	375

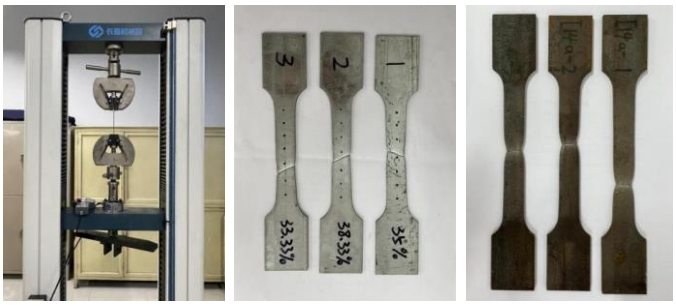

(a)Test device (b)Steel sheet after tensile test (c) Channel steel after tensile test

Fig. 3 Steel tensile test

The material properties of rigid polyurethane foam refer to the relevant provisions in Chinese standards GB / T 21558 - 2008[31] and GB / T 8813 - 2020[32], and are calculated according to the formula in Reference [33], the formulas are as follows:

Elastic modulus:

$$E = 4.6 \times (\rho / 38)^2 \tag{1}$$

Shear modulus:

$$G = 1.725 \times (\rho / 38)^2 \tag{2}$$

Compressive strength:

$$f_y = 0.15 \times (\rho / 38)^{3/2} \tag{3}$$

Shear strength:

$$f_y = 0.078 \times (\rho / 38)^{3/2} \tag{4}$$

After calculation, the properties of polyurethane foam can be obtained, as shown in Table 2.

Table 2
Mechanical properties of rigid polyurethane foam

Compressive strength/MPa	Compression modulus/MPa	Shear strength/MPa	Shear modulus/MPa	Poisson's ratio
0.38	15.61	0.20	5.85	0.3

3.3. Loading device and procedure

In the test, the self-balancing gantry reaction frame and the hydraulic actuator are used to apply a load, and the monotonic static force is evenly

distributed at the third point positions of the sandwich slab through the secondary distribution beam. To avoid the load-acting direction not perpendicular to the test piece plane due to the downward deflection of the specimen, the single-span hinge supports are placed at both ends of the distribution beam. Both ends of the specimen are equipped with sliding and fixed hinge supports to ensure that the sandwich floor can move horizontally. Among them, a round steel with a diameter of 50mm is in direct contact with the steel sheet as the sliding hinge support and another round steel is welded to the steel sheet as the fixed hinge support. At the same time, 20mm steel plates are placed at the supports of the sandwich slab to avoid local damage to the specimen caused by stress concentration. The test loading device is shown in Fig. 4 and Fig. 5

Before the test was officially loaded, 10 kN was applied for preloading to check whether the supports and all the instruments were working properly, and then the test was officially loaded after unloading. The load control method was used for staged loading, and before the maximum deflection of the sandwich slab reached 1/200 of the slab span (elastic limit stage), the load for each level was 10kN. After that, the load was applied at each level of 5 kN, and the loading was stopped until the specimen was destroyed and could not continue to bear the load. Real-time monitoring is carried out through force sensors during the test process, and test data is collected using the DHDAS dynamic signal acquisition system. When the specimen exhibits obvious failure or the beam end load drops to 85% of the peak load, it is considered specimen failure and the test is terminated.

Fig. 4 Loading device

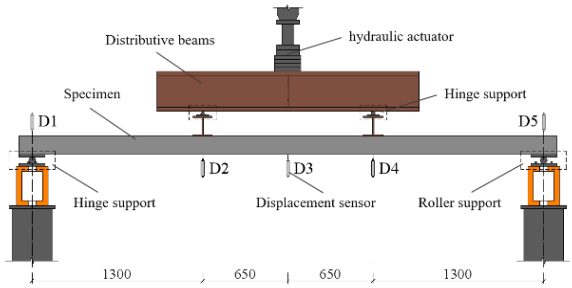

Fig. 5 Sketch of loading device

3.4. Experiment results and analysis

3.4.1. Failure process

The deflection deformation of the specimen was small at the initial stage of loading. When the load increased to 0.4*Pu*, the mid-span deflection was 19.5mm, and the deflection was 1/200 of the span, reaching the limit value of the normal service limit state of the sandwich slab. At this time, there was, a slight sound inside the sandwich slab, but the specimen had no obvious deformation, as shown in Fig. 6(a). When the load increased to about 0.7*Pu*, a continuous "creak" sound began to emit inside the specimen, the deflection of the sandwich slab grew rapidly and a significant bending deformation occurred, as shown in Fig. 6(b). Subsequently, with a small increase in the load value, the deflection of the specimen increased rapidly. When the load increased to *Pu*, the midspan deflection reached 93.4mm and the deflection was about 1/42 of the span. The midspan position of the channel steel was more affected by the bending moment, and the flange bulged outward due to local buckling, the specimen reached the ultimate bearing capacity state, as shown in Fig. 6(c).

（a）Initial state of the specimen

（b）Intermediate state of the specimen

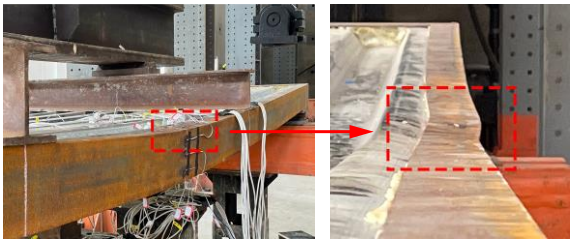

（c）Final failure state of the specimen

Fig. 6 Loading and failure process of the specimen

3.4.2. Deflection

The load-deflection curve of the sandwich slab at the midspan is shown in Fig. 7, where the load value does not include the self-weight of the specimen, and the deflection value is corrected by the displacement of the supports (the corrected deflection value = the deflection values at the midspan and the loading points minus the support displacement value).

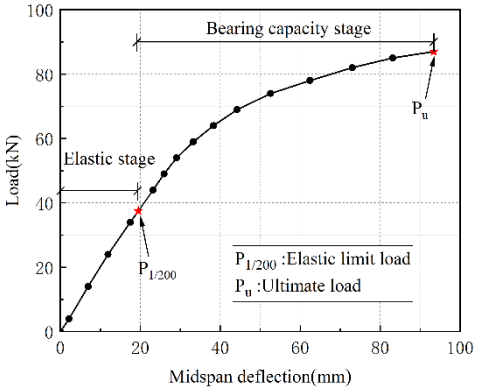

Fig. 7 Midspan load-deflection curve of sandwich slab

From the load-deflection curve at midspan, it can be seen that the load and deflection of the sandwich slab change linearly at the initial stage of loading, the stiffness of the specimen remains unchanged, about 1.9kN/mm. When the sandwich slab is loaded to the elastic limit load, the curve still maintains a linear relationship, indicating that the sandwich slab is in an elastic state during the elastic limit state. As the load increases, the channel steel at the midspan yields, the curve turns, and the stiffness of the specimen decreases slightly, the stiffness is about 1.2kN/mm, while the load value continues to rise, indicating that the profiled steel plate and the polyurethane core layer continues to function. When the specimen is damaged, the lower tensile steel sheet and the channel steel both reach the yield state.

4. Numerical simulation

4.1. Finite element model

In the model of PSSPSS, there are five main components: profiled steel .accurately simulate the actual components in the model, appropriate unit types should be selected based on their cross-sectional and material characteristics.

Based on the test, the geometric dimensions, material properties, loading scheme, and boundary conditions of the finite element model are consistent with the test specimen. In the model, the profiled steel sheet is equipped with a four-node reduced-integration shell element (S4R), while the channel steel and polyurethane sandwich has an eight-node hexahedral reduced-integration solid element (C3D8R). The core layer is made of polyurethane foam, which is closely bonded with steel sheet and channel steel to ensure cooperative work in the test, so the tie is used between the profiled steel sheet, channel steel, and core layer. In order to avoid local damage to the model caused by stress concentration, the steel backing plates are set at the loading point, and the supports, and bound with the contact of the sandwich slab. The loading point is coupled with the steel backing plate, and the two points are loaded symmetrically with displacement control. The boundary conditions at both ends of the sandwich slab are hinged, one end constrains U1, U2, U3, UR2, UR3, and the other end constrains U1, U2, UR2, UR3. Using the structured grid control method, the model is divided into regular grid cells, and the size is selected as 0.02m. The finite element model is shown in Fig. 8. Based on the test, the geometric dimensions, material properties, loading scheme, and boundary conditions of the finite element model are consistent with the test specimen. In the model, the profiled steel sheet is equipped with a four-node reduced-integration shell element (S4R), while the channel steel and polyurethane sandwich has an eight-node hexahedral reduced-integration solid element (C3D8R). The core layer is made of polyurethane foam, which is closely bonded with steel sheet and channel steel to ensure cooperative work in the test, so the tie is used between the profiled steel sheet, channel steel, and core layer. In order to avoid local damage to the model caused by stress concentration, the steel backing plates are set at the loading point, and the supports, and bound with the contact of the sandwich slab. The loading point is coupled with the steel backing plate, and the two points are loaded symmetrically with displacement control. The boundary conditions at both ends of the sandwich slab are hinged, one end constrains U1, U2, U3, UR2, UR3, and the other end constrains U1, U2, UR2, UR3. Using the structured grid control method, the model is divided into regular grid cells, and the size is selected as 0.02m. The finite element model is shown in Fig. 8.

The finite element model employs rigid polyurethane foam as an isotropic material, the ideal elastoplastic model as the constitutive model, and the double broken line model as the constitutive model of steel. Refer to Table 1 and Table 2 for each parameter.

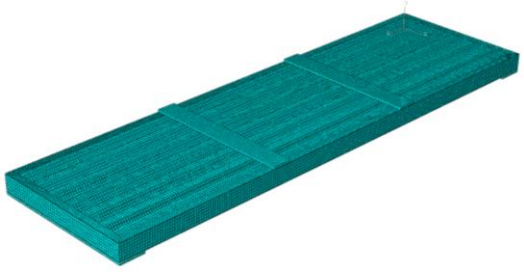

Fig. 8 Finite element model

4.2. Numerical simulation results and analysis

Table 3 displays a comparison between the test data and finite element calculations of the bearing capacity under elastic and bearing capacity limit states. Fig. 9 shows the comparison of midspan load-deflection curves of the sandwich slab obtained from FEA and test. It can be seen that the overall changing trends of the two load-deflection curves are basically the same, and the differences between the normal service load and the failure load of the two curves are all small, the differences are 5.7% and 3.3%, respectively. Due to the possible nonuniformity of the polyurethane foaming density, the uncertainty of the properties of the polyurethane material is caused, which makes the properties of the polyurethane material in the finite element model deviate from the test piece. Secondly, the boundary conditions in the finite element model cannot be guaranteed to be completely consistent with the support conditions in the test, and the manual data collection will also cause a deviation in the results. Finally, there are errors between the finite element simulation results and the experimental results.

Table 3
Comparison of experimental and numerical simulation results

Bearing capacity	Test value/kN	numerical simulation value/kN	Ratio/%
$P_{1/200}$	37.50	35.49	5.70
P_u	87.00	84.34	3.20

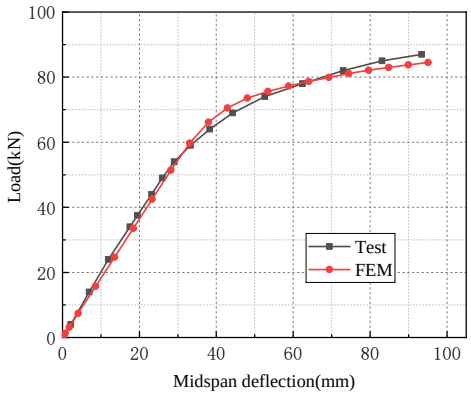

Fig. 9 Comparison of load-deflection curves

In addition, When the specimen reaches its maximum bearing capacity, the mid-section of the channel steel buckles and bulges outward. The sandwich slab's failure characteristics, as seen in Fig.10, were found to agree with those from the test, in comparison to the finite element simulation. Therefore, the finite element model proposed in this paper can better simulate the flexural performance of the sandwich slab.

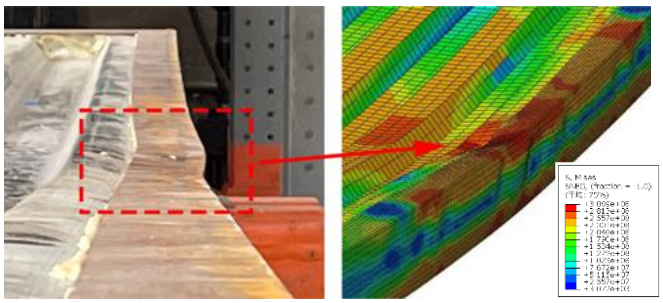

Fig. 10 Comparison of test and FEM failure characteristics

4.3. Parametric analysis

To further study the flexural mechanical properties of the profiled steel sheet-polyurethane sandwich slab, based on the test results and FEA results of the sandwich slab in Section 3.1 and Section 4.1, the parametric analysis of the sandwich slab is carried out to obtain the influence of various factors on the flexural performance of the sandwich slab. The parameters are shown in Table 4.

Table 4
Variation of parameters of sandwich slabs

Geometry			Material
Slab thickness/mm	Slab span/mm	Steel sheet thickness/mm	PU density/(kg·m^{-3})
120	2700	1	45
140	3300	1.5	65
160	3900	2	75
180	4500	2.5	90
200	5100	3	—

4.3.1. Slab thickness

Fig.11 reveals that, with a rise in slab thickness, the bearing capacity and stiffness of the sandwich slab are significantly enhanced, with an even greater increase. This is evidenced by the comparison of load-deflection curves and

finite element calculation results. Compared with the slab thickness of 120mm, when the slab thickness is 200mm, the flexural capacity of the sandwich slab is increased by 267% under the limit state of elastic, and 172% under the ultimate state of bearing capacity.

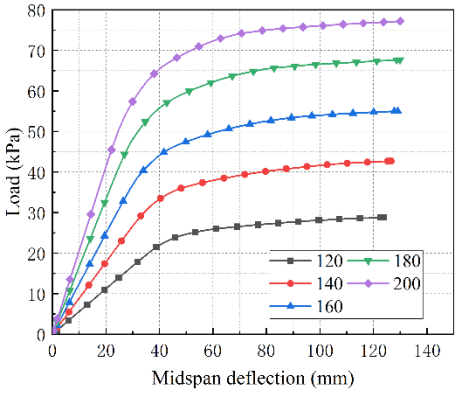

Fig. 11 Load-deflection curves of slab thickness variations

4.3.2. Slab span

As shown in Fig. 12, by comparing the load-deflection curves and the finite element calculation results of the sandwich slab with different slab spans, it can be found that compared with the slab span of 5100mm, when the slab span is 2 700mm, the flexural capacity of the sandwich slab is increased by 283% under the limit state of elastic, 167% under the limit state of bearing capacity. The sandwich slab's bearing capacity and stiffness are significantly enhanced, and the alteration of the slab span has a more noticeable impact on the slab's flexural bearing capacity when it is in the under-the-limit state of elasticity. As the slab span is reduced, the bearing capacity and stiffness of the sandwich slab are progressively increased, and the stiffness turning point is gradually advanced, thus increasing the stiffness of the sandwich slab.

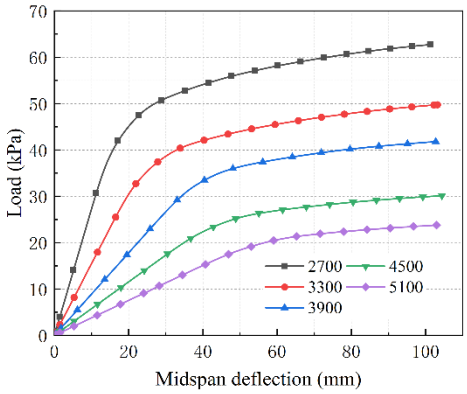

Fig. 12 Load-deflection curves of slab span variation

4.3.3. Profiled steel sheet thickness

Fig. 13 shows the influence of the profiled steel sheet thickness on the load-deflection curve of the sandwich slab. It can be seen from Fig. 13 that the bearing capacity and stiffness of the sandwich slab improved significantly with the increase of the profiled steel sheet thickness. When it is increased from 1mm to 3mm, the bearing capacity of the sandwich slab increases by 127 % in the elastic limit state and 187 % in the bearing capacity limit state. It can be seen that when the profiled steel sheet is thin, the corresponding load-deflection curve changes abruptly when the deflection is large. Compared with the corresponding finite element program, it is found that the compressed steel sheet buckles at the midspan, which can indicate that the thinner profiled steel sheet will change the failure mode of the sandwich slab.

4.3.4. Polyurethane foam density

The influence of rigid polyurethane foam density on the load-deflection curve of the sandwich slab is shown in Fig. 14. It can be seen that with the increase of polyurethane density, the bearing capacity and stiffness of sandwich slab have been improved to a certain extent, but the improvement is not obvious. The elastic limit state of the sandwich slab bearing capacity rises 26% when the density shifts from 45kg/m³ to 90kg/m³, and 15% when it reaches its ultimate state.

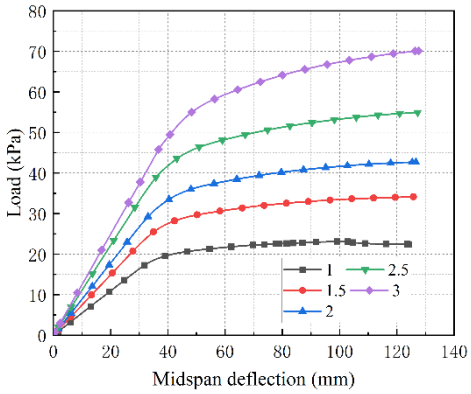

Fig. 13 Load-deflection curves of profiled steel sheet thickness variation

5. Calculation of slab deflection and flexural capacity

The shear modulus of the core material, with its special structural form, is minuscule, and when compressed, it will cause considerable shear deformation; thus, the shear deformation of the core material cannot be overlooked. The flexural stiffness of the core material is minimal, and its contribution to the bending deformation resistance can be disregarded[17]. Therefore, the bending deformation of the sandwich slab is mainly controlled by steel sheet and channel steel, and the shear deformation is shared by steel sheet, channel steel, and core material.

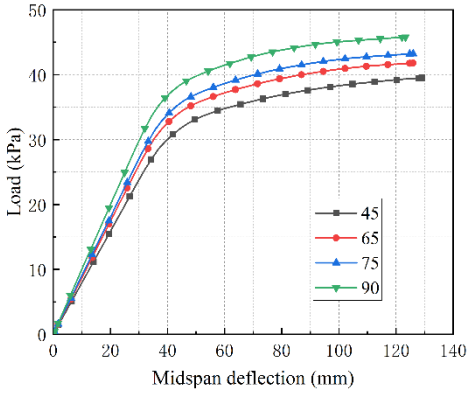

Fig. 14 Load-deflection curves of polyurethane foam density variation

5.1. Approximate calculation of slab stiffness

For a deep-profiled steel sheet, its flexural rigidity needs to be considered, while for polyurethane, the influence of the stiffness of the core layer on the sandwich slab cannot be considered. Therefore, the flexural rigidity of PSSPSS to the neutral axis is mainly determined by the stiffness of the profiled steel sheet itself, the stiffnesses of the profiled steel sheet, and the channel steel to the neutral axis of the sandwich slab.

Flexural rigidity of sandwich slab：

$$K = EI_1 + EI_2 + EI_3 \tag{5}$$

Where K is the total stiffness of the sandwich slab; EI_1 is the stiffness of the profiled steel sheet itself; EI_2 is the stiffness of the profiled steel sheet to the neutral axis of the sandwich slab; EI_3 is the stiffness of channel steel to the neutral axis of the sandwich slab.

5.2. Equivalent thickness and equivalent shear modulus of the core layer

Fig. 15 is the cross-sectional diagram of PSSPSS. According to the cross-sectional characteristics of the deep-profiled sandwich slab, the following relationship can be obtained:

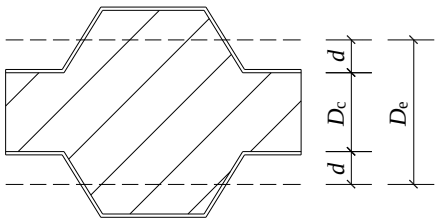

Fig. 15 Diagram of a cross-section of sandwich slab

Effective core thickness:

$$D_e = D_c + 2d \tag{6}$$

Effective cross-sectional area:

$$A_e = A_c D_e / D_c = A_c \left(D_c + 2d\right) / D_c \tag{7}$$

Effective shear modulus:

$$G_e = G_c D_e / D_c = G_c \left(D_c + 2d\right) / D_c \tag{8}$$

Where D_c is the core thickness (mm); A_e is the cross-sectional area of the core layer (mm^2); G_e is the shear modulus of core material (MPa); d is the distance from the centroid axis of profiled steel sheet to the flange edge of steel sheet (mm).

5.3. Calculation of deflection under uniform load

Based on the experimental study, finite element comparative verification, and finite element variable parameter analysis of PSSPSS, according to the calculation formula of the sandwich slab in Chinese standard GB/T 23932 - 2009[34] and the theory of sandwich beam, the deflection calculation formula of the sandwich slab is theoretically deduced, and the formula is as follows:

$$\omega = \frac{5qL^4}{384K} + \frac{k\beta qL^2}{8A_e G_e} \tag{9}$$

Where L is the span of the sandwich slab (mm); K is the flexural rigidity of the sandwich slab; k is the non-uniformity coefficient of shear stress (1.2 for rectangular section); β is the shear distribution coefficient; A_e is the cross-sectional area of the core layer (mm^2); G_e is the shear modulus of core material (MPa).

The deflection of the sandwich slab calculated by the above formula is 19.9mm, and the finite element simulation value is 19.5mm. The theoretical calculation value is higher than the finite element result, and the error is only 2.1%, which shows that the theoretically derived formula can be used to calculate the deflection of PSSPSS in the elastic limit state.

5.4. Calculation of flexural capacity under uniform load

The flexural capacity of the sandwich slab is mainly controlled by the deformation during the elastic limit state. When the plate deflection reaches l/200, the flexural bearing capacity of PSSPSS under uniform load can be determined by the following formula, which generally dictates that the maximum deflection of the sandwich slab should not exceed 1/200 of the slab span.

$$q = \frac{\omega}{\dfrac{5L^4}{384K} + \dfrac{k\beta L^2}{8A_e G_e}} \tag{10}$$

The flexural bearing capacity of the sandwich slab with different parameters in the elastic limit state is calculated and compared with the FEA results, which are based on the calculation formula of flexural capacity of the sandwich slab under uniform load. The calculated flexural capacities are compared with the FEA results, as shown in Fig. 16. The results of the proposed equations are in agreement with the FEA results, with errors of only 10% being observed. The errors are only about 10%. This means that the formula has good applicability.

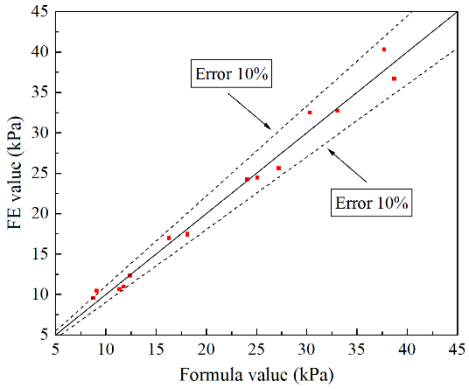

Fig. 16 Error distribution of flexural bearing capacity formula and simulation results

6. Conclusion

Using ABAQUS software for finite element analysis and variable parameter analysis, this article designs and manufactures a set of experimental components for static test research, utilizing the PSSPSS as the research object. Subsequently, the results of the experiment and finite element analysis are used to derive the deflection calculation formula and flexural bearing capacity calculation formula of the sandwich panel, leading to the following conclusions:

(1) The mid-span deflection of the sandwich slab is too large when damaged, reaching a maximum of 93.4mm - approximately 1/42 of the span. The tensile profiled steel panel and channel steel have both reached the yield state, and the mid-span position of the channel steel is deformed and buckled. However, due to the supporting effect of the deep corrugations of the profiled steel plate and the core layer, the buckling resistance of the metal surface layer is increased, so that the buckling of the profiled steel sheet does not occur.

(2) The experimental data and numerical simulation results, when compared, demonstrate that bearing capacity errors are minimal under normal service load and failure load, at 5.7% and 3.3%, respectively. Simulation of the sandwich slab failure characteristics and stress by the finite element method yielded results that were in perfect harmony with the experimental ones, demonstrating the finite element model's capability of accurately replicating the sandwich slab's mechanical performance and confirming the accuracy of the experimental results.

(3) The sandwich slab bearing capacity is significantly affected by the slab thickness, profiled steel sheets thickness, and span, whereas the density of polyurethane foam and stiffeners has no major effect. With the increase of plate thickness and profiled steel plate thickness, the flexural bearing capacity of sandwich panels is significantly improved. The reduction of plate span has a more significant effect on the flexural bearing capacity of panels under normal use. The increase of polyurethane foam density slightly improves the bearing capacity of sandwich panels.

(4) Additionally, for the calculation of the deflection of sandwich slabs, a calculation formula is derived based on existing theories and compared with experimental results, with an error of only 2.1%, verifying the correctness of the formula; Based on the formula for calculating the deflection of sandwich slabs, a formula for calculating the flexural bearing capacity of sandwich slabs is derived. The results of the calculation of the bearing capacity of sandwich slabs with different parameters are compared with the results of finite element analysis. The maximum error is 9.97%, indicating that the proposed formula for flexural bearing capacity has certain applicability.

Acknowledgments

This research was funded by the Local Science and Technology Development Fund Project Guided by the Central Government (206Z7601G) and the Natural Science Foundation of Hebei Province (E2020210074 & E2022210084).

References

[1] Lawson RM, Ogden RG, et al. Application of modular construction in high-rise buildings [J]. 2012, 18(2): 148-54.
[2] Faidzi MK, Abdullah S, Abdullah M F, et al. Review of current trends for the metal-based sandwich panel: Failure mechanisms and their contribution factors [J]. Engineering Failure Analysis, 2021, 123: 105302.
[3] Noor AK, Burton WS, Bert CW. Computational models for sandwich panels and shells[J]. Appl Mech Rev, 49(3), 1996.

[4] Mugahed Amran YH, Raizal SM. Rashid and Farzad Hejazi. Response of precast foamed concrete sandwich panels to flexural loading[J]. Journal of Building Engineering 2016, 7: 143–158.
[5] Mugahed Amran YH, Abang Ali AA, Rashid R SM, et al. Structural behavior of axially loaded precast foamed concrete sandwich panels [J]. Construction and Building Materials, 2016, 107: 307-20.
[6] Choe J, Huang Q, Yang J, et al. An efficient approach to investigate the post-buckling behaviors of sandwich structures [J]. Composite Structures, 2018, 201: 377-88.
[7] Huang Q, Choe J, Yang J, et al. An efficient approach for post-buckling analysis of sandwich structures with elastic-plastic material behavior [J]. 2019, 142: 20-35.
[8] Huang Q, Choe J, Yang J, et al. The effects of kinematics on post-buckling analysis of sandwich structures [J]. 2019, 143: 106204.
[9] Aktham Alchaar and Farid Abed. Finite element analysis of a thin-shell concrete sandwich panel under eccentric loading[J]. Journal of Building Engineering 2020.
[10] Hartsock JA. Design of Foam-Filled Structures[D]. Technomic, Stamford, Connection, 1969.
[11] Hartsock JA, Chong KP. Analysis of sandwich panels with formed faces, Proc[J]. ASCE. J. Strcuc. Div., 102(ST4), 1976.
[12] Chong KP, Wang KA, Griffith GR. Analysis of continuous sandwich panels in building systems[J]. Building and Environment, 1979, 14(2): 125-130.
[13] Allen HG. Sandwich panels with thick or flexurally stiff faces, Sheet Steel in Building, Proc[J]. Mtg Iron and Steel Institute, RIBA, March 1972.
[14] Allen HG. Sandwich construction[D]. University of Southampton, Department of Civil Engineering, Report CE/1/72, January 1972.
[15] K.M.A. Sohel and J.Y. Richard Liew. Steel-concrete-steel sandwich slabs with lightweight core - Static performance[J]. Engineering Structures 2011; 33: 981–992.
[16] K.M.A. Sohel and J.Y. Richard Liew. Behavior of steel-concrete-steel sandwich slabs subject to impact load[J]. Journal of Constructional Steel Research 2014; 100: 163–175.
[17] Davies JM. Sandwich panels[J]. Thin-walled structures, 1993, 16(1-4): 179-198.
[18] Davies JM. Design Criteria for Structural Sandwich Panels[J]. The Structural Engineer，1987.65A(12): 435~441.
[19] Davies JM. Lightweight Sandwich Construction[J]. CIB Working Commission PP.195~215.82~140.
[20] Chong KP and Hartsoek JA. Structural analysis and design of sandwich panels with cold-formed steel facing[J]. J Thin-Walled Struct 1993; 16: 79–96.
[21] Russo A and Zuccarello B. Experimental and numerical evaluation of the mechanical behavior of GFRP sandwich panels[J]. Compos Struct 2007; 81: 575–586.
[22] Ramtekka GS, Desai YM and Shah AH. Application of a three-dimensional mixed finite element model to the flexure of sandwich plate[J]. Comput Struct 2003; 81: 2183–2196.
[23] Ramtekkar G, Desai Y, et al. Mixed finite-element model for thick composite laminated plates [J]. 2002, 9(2): 133-56.
[24] Kachalla Mohammeda, Izian Abd Karima, and Rasheed Abed Hammood. Composite slab strength determination approach through reliability analysis[J]. Journal of Building Engineering 2017; 9: 1–9.
[25] Mohammed K, Karim IA, Aziz F. Composite Slab Numerical Strength Test Method Under Partial Connection Approach; proceedings of the GCEC 2017: Proceedings of the 1st Global Civil Engineering Conference 1, F, 2019 [C]. Springer.
[26] Davies JM and Hakmi MR. Postbuckling behavior of foam-filled thin-walled steel beams[J]. J Construct Steel Res 1991; 20: 75–83.
[27] Davies JM. Axially loaded sandwich panels[J]. J Struct Eng 1987; 113: 2212–2230.
[28] Mousa MA and Uddin N. Global buckling of composite structural insulated wall panels[J]. Mater Des 2011; 32: 766–772.
[29] Mousa MA and Uddin N. Structural behavior and modeling of full-scale composite structural insulated wall panels[J]. Eng Struct 2012; 41: 320–334.
[30] GB/T 228.1-2010. Metallic materials - Tensile testing - Part 1:Method of test at room temperature[S]. Beijing: China Standards Press, 2010.
[31] GB/T 21558-2008. Rigid polyurethane cellular plastics are used in the thermal insulation of buildings [S]. Beijing: China Standards Press, 2008.
[32] GB/T 8813-2020. Rigid cellular plastics - Determination of compression properties[S]. Beijing: China Standards Press, 2020.
[33] Xiaoxiong Cha. insulation panels for building - metal face and non-metal face[M]. Beijing: Science Press, 2011.
[34] GB/T 23932-2009. Double skin metal faced insulating panels for building[S]. Beijing: China Standards Press, 2009.